Int. J. Electrochem. Sci., 15 **(2020)** 4470 – 4480, doi: 10.20964/2020.05.46

International Journal of
ELECTROCHEMICAL
SCIENCE
www.electrochemsci.org

Electrochemical Evidence of Corrosion Resistance of Polyaniline Film on the Copper Surface

Xinliang Zhang

Mechanic Engineering College, ChongQing Industry Polytechnic College, Yubei District Chongqing, 401120, P.R. China
*E-mail: kangteng92251778@163.com

Received: 22 December 2019 / *Accepted:* 2 February 2020 / *Published:* 10 April 2020

The role of aniline and its derivative polymer films in the field of metal corrosion has attracted extensive attention. The anti-corrosion effect of aniline and its derivative polymer film on iron and its alloy has been reported in the literature. There are few reports on the corrosion protection of aniline and its derivatives to copper. The purpose of this paper is to study the electropolymerization of aniline on copper and its corrosion resistance. The results show that a change in aniline concentration has little effect on the durability of the aniline polymer film. The polyaniline film can only provide a short-term physical barrier to the base metal, and its effect decreases rapidly with increasing immersion time in a corrosive medium.

Keywords: Polyaniline Film; Copper; Sodium Oxalate; Electrodeposition; Open-Circuit Potential

1. INTRODUCTION

The damage to metals or alloys caused by the chemical and electrochemical action of external media is called corrosion. It is generally believed that metals are damaged or deteriorated in the environment due to a combination of chemical, electrochemical and physical dissolution reactions. The process of metal corrosion is a complex multiphase reaction at the interface of the metal and medium, so the damage always goes from the surface of the metal to the interior [1–3]. In the process of corrosion, the appearance of metal changes at the same time, such as the presence of small holes or corrosion products on the metal surface, or the thinning of the metal materials. The mechanical properties and microstructure of metals also change, demonstrating metal embrittlement and strength reduction, and in some cases, a change in content of some elements in the metal or a phase transformation of the metal structure [4–7]. The corrosion of metal has a significant impact on its performance. The damage is not only the metal itself but also the metal structure. Copper has good conductivity, heat conduction and machining properties. It is easy to weld a copper alloy, and it also has excellent seawater corrosion

resistance and stain resistance. Therefore, for a long time, copper and copper alloys were widely used and developed in the industrial, military and civil fields. Copper has high thermal stability; therefore, in general, copper has no corrosion tendency and is listed as a corrosion-resistant metal. However, in water containing oxygen, oxidizing acid and other solutions containing CN^-, NH^{4+}, and Cl^-, which can form complex ions with copper, copper corrosion is more severe [8–14].

In general, the traditional corrosion inhibition of copper is usually provided by a coating. In general, acid pickling and passivation are often used to improve the corrosion resistance of copper and its alloys in a general environment [15–18]. The application of corrosion inhibitors has become an important achievement in the development of corrosion science and corrosion engineering, especially in the development and application of corrosion inhibitors for economic and environmental protection; thus, this technology has been a research hotspot in recent years. There have been many reports over the past few years of the electrochemical deposition of various polymer anticorrosion films on various steel materials, such as stainless steel, low carbon steel, galvanized steel and ferroalloy, including polyaniline and its derivatives [19–24]. Among them, conductive polyaniline and its derivatives have attracted the most attention. Although compared with insulating polymer films, the feasibility of conducting polymer films for metal anticorrosion is still a controversial issue. The research of polyaniline anticorrosive performance started from the electrochemical polymerization of aniline [25–29]. The researchers studied the electrochemical synthesis of polyaniline on iron sheets in alkaline solutions of aniline and sulfuric acid and found that the anticorrosive ability of the film could be as high as 80 h in a salt spray test. The corrosion protection of polyaniline on stainless steel was studied. The open circuit potential method was used to evaluate the corrosion inhibition effect. The corrosion rate of 410 steel is less than 25 μm/a when polyaniline is coated, and the open circuit potential is 0 V in a 1 M sulfuric acid medium at 25 °C. Under the same conditions, the average corrosion rate of the uncoated samples after 64 h of exposure reached 3100 μm/A, which is roughly equivalent to the corrosion rate of the activated metal at approximately -0.5 V. The results show that polyaniline can maintain the passivation potential of stainless steel and keep it in an anodic protection state [30–34]. After that, it is found that polyaniline can passivate the metal surface. Passivation is due to the oxide film formed by the contact between the metal and polyaniline. When the polyaniline film on the metal surface is peeled off, there is a passive film on the metal surface. The active conductive polymer film can not only block the corrosive medium but also has a different protection mechanism from a traditional one [35–42]. The conductive polymer film can make the metal repassivate by a redox reaction at the metal base interface of the film; furthermore, the corrosion resistance of proton-doped polyaniline in an acidic medium is stronger than that in a neutral medium. In view of the excellent performance of polyaniline film in the field of corrosion protection of iron and iron products, this paper prepares polyaniline in a neutral sodium oxalate solution. The formation of a polyaniline film and its corrosion protection effect on copper metal is analyzed with open circuit potential measurements, potentiodynamic polarization curves and AC impedance measurements.

2. EXPERIMENTAL

Aniline and sodium oxalate were purchased from Sinopharm Ltd. Copper discs were purchased from a local supermarket. A mixed solution of 0.1 M NaOH and 0.2 M Na_2SO_4 was used as the

electrolyte. Solutions of 0.2 M sodium oxalate+0.15 M aniline, 0.2 M sodium oxalate+0.1 M aniline, 0.2 M sodium oxalate+0.05 M aniline and 0.1 M sodium oxalate+0.1 M aniline were used for polyaniline film deposition. All electrochemical tests were performed with a CHI600B electrochemical working station. The corrosion resistance of the composite film-coated samples was estimated by a potentiodynamic polarization curve and electrochemical impedance spectroscopy (EIS) measurements. A working electrode, auxiliary electrode (Pt) and reference electrode (Ag/AgCl) constituted the three-electrode system. The potentiodynamic curves were obtained using an electrochemical analyzer from -100 mV to 100 mV vs the open circuit potential (OCP) at a constant voltage scan rate of 0.5 mV/s. EIS measurements were conducted over a frequency range of 100 kHz to 10 mHz with a sinusoidal amplitude of 10 mV. Prior to each electrochemical test, a stabilization period of 1800 s was applied.

3. RESULTS AND DISCUSSION

First, the components of the electrolyte to be selected were tested by cyclic voltammetry to investigate the CV behavior of each component. At the same time, a comparison was made between the platinum electrode and the copper electrode to distinguish whether the voltammetric peak was the oxidation-reduction of copper. Figure 1A shows the CV curves of the platinum electrode and copper disk electrode in a 0.2 M sodium oxalate aqueous solution. It can be seen from curve a that there is almost no current passing through the platinum electrode before 1.1 V, and the oxygen evolution reaction is initiated after 1.1 V, indicating that sodium oxalate does not undergo an oxidation reaction on the platinum electrode [43,44], and the platinum electrode itself is stable. It can be seen from curve B that the oxidation current gradually increases at approximately -0.1 V on the copper electrode and reaches the maximum value at approximately 0.75 V, which is attributed to the oxidative dissolution or formation of an oxide film on the copper electrode. This current peak is obviously a compound peak, which contains the complex oxidation reaction of copper. This result indicates that the growth of the inhibiting film on the metal surface interferes with the charge transfer process [45]. Interestingly, when the potential sweeps back, an anodic peak is formed at approximately 1.3 V. It is generally believed that oxalate ions in a sodium oxalate solution react with copper to form a kind of water-insoluble copper oxalate coating on the surface of the copper metal. The copper oxalate has weak conductivity, but there is no stable potential region with a high passivation degree in Figure 1A.

In the aqueous solution of aniline without a supporting electrolyte, due to the small conductivity of the solution, the current is very small both on the copper disk electrode and on the platinum plate electrode (Figure 1B). In contrast, the current on the platinum electrode is small, and the reduction current is almost zero. A black film can be seen on the platinum plate after the reaction, which indicates that the oxidation of aniline to a polyaniline film on the surface of platinum is irreversible [46,47]. The current on the copper electrode is much higher than that of the platinum electrode. After the reaction, a polyaniline film cannot be seen on the surface of copper, indicating that aniline does not directly form a polymer film on the surface of copper, but rather, a compound of aniline copper. The copper compound is reduced during a subsequent negative (reduction) scan.

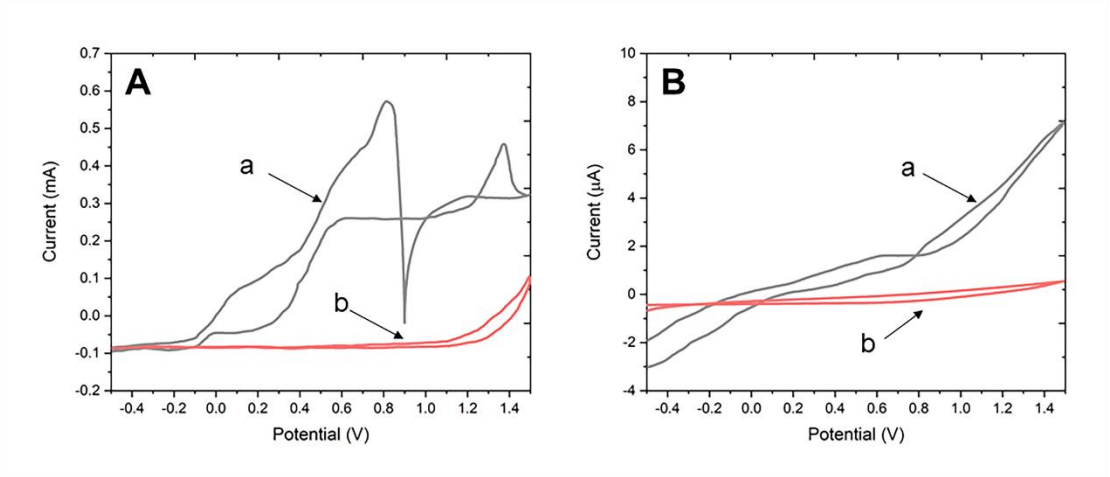

Figure 1. (A) CV curves of the (a) platinum and (b) copper disk electrodes in a sodium oxalate solution (0.2 M, scan rate: 20 mV/s). (B) CV curves of the (a) platinum and (b) copper disk electrodes in an aniline solution (0.15 M, scan rate: 20 mV/s).

Figure 2A shows the CV curves of different electrodes in a solution of sodium sulfate and aniline. It can be seen from the figure that on the CV curve (curve a) of the platinum electrode, there is an obvious oxidation peak at 1.0 V, and a layer of black polyaniline film is formed on the electrode after the end of the cyclic voltammetry test. In contrast, on the copper electrode, there is an electric current from the beginning, and then it almost appears with a positive shift of electric potential. The increase of linearity and the decrease of inverse sweep are similar to the behavior of pure resistance. At the end of one cycle of scanning, the polyaniline film formed on the copper electrode is not black, but rather, a yellow green copper compound, which also shows that the polyaniline protective film cannot be directly formed on the surface of copper.

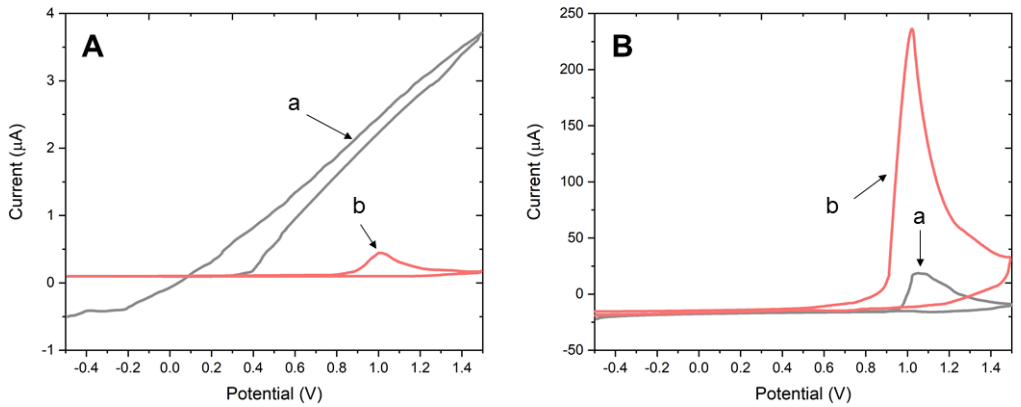

Figure 2. (A) CV curves of the (a) platinum and (b) copper disk electrodes in a sodium sulfate (0.2 M) and aniline solution (0.15 M, scan rate: 20 mV/s). (B) CV curves of the platinum in an aniline solution (0.15 M) with (a) sodium oxalate (0.2 M) and (b) sodium sulfate (0.2 M) as the electrolyte (scan rate: 20 mV/s).

Figure 2B shows the CV diagram of aniline on the platinum electrode after adding 0.2 M sodium oxalate and 0.2 M sodium sulfate to a 0.15 M aniline aqueous solution. It can be seen that aniline has an

obvious anodic peak at approximately 0.1 V, and the peak current in the sodium sulfate solution is approximately 10 times that in the sodium oxalate solution. A black polyaniline film is formed on the platinum plate after the reaction, which indicates that this peak is the peak of the polyaniline polymer film [48–50]. However, judging from the electric quantity of the peak, the thickness of the film is closely related to the properties of the supporting electrolyte.

Figure 3 shows the cyclic voltammetry curves of the platinum and copper plate electrodes in an aqueous solution of sodium anilinolate. Curve a is the redox reaction on the platinum electrode. It has been confirmed that the oxidation of sodium oxalate does not take place on the metal platinum. The small anodic peak near 1.0 V is the polymerization peak of aniline. Curves b and c are the CV curves of the sodium oxalate solutions with and without aniline on the copper disk electrode, respectively. Compared with curve a, the high and broad compound oxidation peak between 0-1 V in curves b and c should be the process of copper oxidation and its combination with oxalate to form a passive film [51–54]. Previous studies indicate that a refined grain size plays a positive role in corrosion behavior, including inducing improvements in intergranular and pitting corrosion resistance [55,56]. The possible mechanism is that a copper oxide film and copper oxalate film are formed on the surface of copper. Compared with line b and line c, it can be seen that the presence of aniline reduces the current plateau to a very low current. In this potential area, aniline may polymerize on the electrode, although the amount of aniline polymerization is very small judging from the current size. The presence of blocked pores in the formed copper oxalate film makes the current plateau no longer appear in curve b in the high potential area [57–60]. Similarly, the current in the reverse scanning process is greatly suppressed by the aniline polymer. When sodium oxalate is added to the solution, the formation of a copper oxalate film on the electrode enables aniline to polymerize on its surface to form a polyaniline film, which passivates the electrode to a large extent. In the absence of sodium oxalate, aniline cannot be polymerized on the surface of copper, which may be related to the anodizing reaction of copper itself. Because the surface condition of copper is constantly changing, aniline molecules cannot be polymerized and deposited on the surface of copper. This situation is avoided on the stable platinum surface so that a polyaniline film of aniline can be formed.

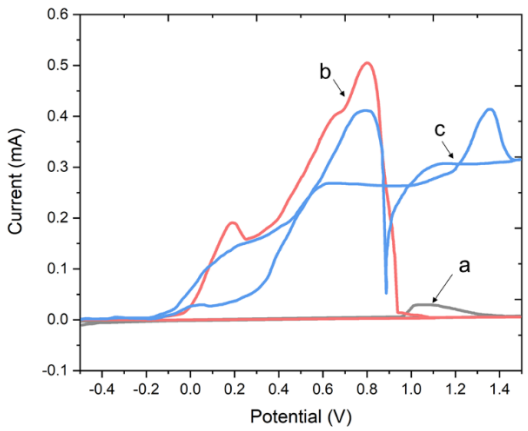

Figure 3. CV curves of the (a) platinum and (b, c) copper disk electrodes in a sodium sulfate (0.2 M) and aniline solution (0.15 M, scan rate: 20 mV/s).

After the copper electrode was formed in the aqueous solution of sodium oxalate with different concentrations of aniline, it was transferred to an aqueous solution of 3% NaCl to test the effect of changes in aniline concentration on the corrosion resistance of the polyaniline film. It can be seen from the curve of film formation with different concentrations of aniline in Figure 4A that with a decrease in aniline concentration, the peak current after the first cycle of the CV curve of film formation gradually increased, and the reverse scanning also opens with a decrease in concentration. An initial peak current is generated, which means that copper can still be dissolved through the oxide film and oxalate film at this time, that is to say, the density of the polyaniline film will also decrease when the concentration of aniline decreases. From the open circuit potential diagram of the polyaniline film prepared in different concentrations of aniline in the 3% NaCl solution in Figure 4B, when a layer of polyaniline film is formed on the electrode surface, the open circuit potential starts to be very high, with values above - 100 mV. When immersed in the 3% NaCl solution, the open circuit potential decreases rapidly, and then it can be reduced to a stable potential in approximately 15 minutes, which is basically the same as the open circuit potential of the copper oxide and oxalate film formed in the pure sodium oxalate solution [61,62]. The stable potential of films formed by different concentrations of aniline is basically the same, and the potential will not decrease with the extension of immersion time, which shows that the concentration of aniline has an effect on the polyaniline film. The effect of durability on corrosion resistance is not significant.

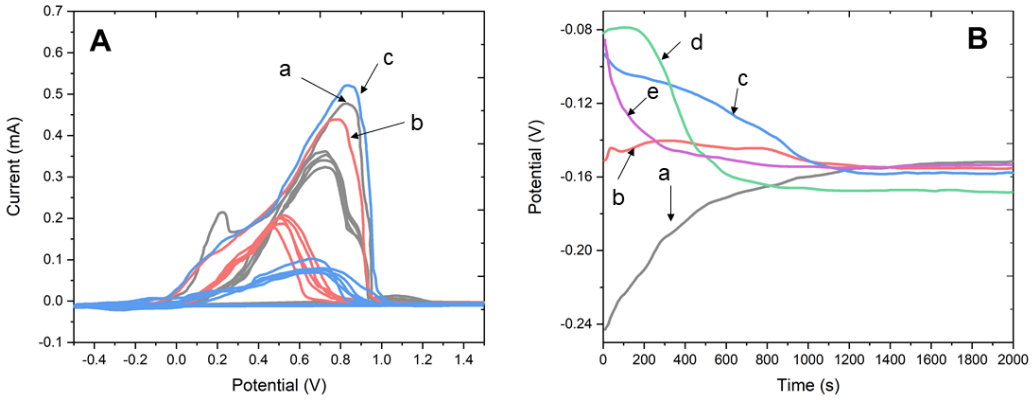

Figure 4. (A) CV curves of the electrochemical deposition of polyaniline: (a) 0.15 M, (b) 0.1 M and (c) 0.05 M aniline solutions (scan rate: 20 mV/s). (B) Open circuit potential diagram of polyaniline films prepared from different concentrations of aniline: (a) copper disk (b) in 0.2 M sodium oxalate, (c) 0.2 M sodium oxalate+0.15 M aniline, (d) 0.2 M sodium oxalate+0.1 M aniline, and (e) 0.2 M sodium oxalate+0.05 M aniline (scan rate: 0.5 mV/s).

Figure 5 shows the impedance diagram and potentiodynamic polarization curves of the polyaniline film prepared in different concentrations of aniline in solution. It can be seen from Figure 5A that the corresponding arc of the polyaniline film prepared in different concentrations of aniline solution in the Nyquist diagram is basically the same. Their intercept on the transverse axis is basically the same. Theoretically, the intercept of the arc on the transverse axis corresponds to the film resistance,

and the greater the film resistance is, the greater the corrosion resistance. This shows that the corrosion resistance of these films is basically the same. It can be seen from Figure 5B that the potentiodynamic polarization curves of these kinds of films are almost the same, and the corresponding corrosion potential corrosion current is also similar, which further shows that the concentration of aniline has little effect on the corrosion resistance of polyaniline films. At the same time, it can be seen from curve a in the two figures that the corrosion resistance effect of the electrode covered by a polyaniline film after soaking in the corrosion solution for a period of time is not better than that of the electrode not covered by a polyaniline film, indicating that a polyaniline film can only provide a physical barrier and has poor stability [63–65]. The corrosion potential (Ecorr), current density (jcorr) and their corresponding anodic/cathodic Tafel slopes (ba and bc) are derived directly from the polarization curves by a Tafel region extrapolation, which are listed in Table 1. The corrosion resistance performance is also compared to those reported by previous studies. The result illustrates that the anodic dissolution process is weakened for the polyaniline film [66]. The results also show that the enhanced crosslinking density of the film inhibits the process of dissolved oxygen reaching the interface of the substrate/film [45].

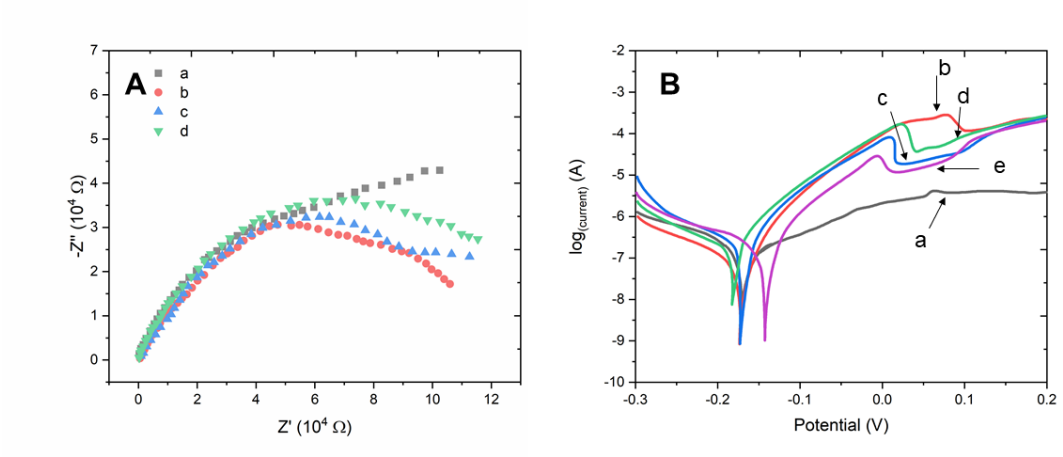

Figure 5. (A) Nyquist plots (amplitude: 10 mV; stabilization period: 1800 s) and (B) potentiodynamic polarization curves (scan rate: 0.5 mV/s) of polyaniline films prepared in different concentrations of aniline: (a) copper disk (b) in 0.2 M sodium oxalate, (c) 0.2 M sodium oxalate+0.15 M aniline, (d) 0.2 M sodium oxalate+0.1 M aniline, and (e) 0.2 M sodium oxalate+0.05 M aniline.

Table 1. Corrosion parameters obtained by Tafel extrapolation method from polarization curves.

Sample	ba (mV/decade)	bc (mV/decade)	Corrosion current density (A/cm^2)	Corrosion potential (V)
a	146	-171	3.225×10^{-5}	-0.213
b	128	-144	7.547×10^{-6}	-0.206
c	121	-122	7.331×10^{-6}	-0.202
d	106	-109	8.206×10^{-6}	-0.196
e	100	-85	7.206×10^{-5}	-0.192

The polyaniline film formed at a high scan rate is very unstable and basically does not play a protective role. In the following experiments, the protective effect of the aniline film formed on the copper sheet during slow scanning was studied. Figure 6a is the CV diagram of the film formed under a slow scanning of 5 mv/s in different concentrations of aniline and sodium oxalate solution. It can be seen from the figure that the peak current decreases with decreasing scan rate, but the peak current decreases disproportionately compared with that of the previous 20 mV/s scanning. The peak shape basically remains unchanged, which means that the film formed at this time is basically the same as the previous one, that is, the oxide and oxalate passivation film of copper is still formed first, and then on this basis, a layer of polyaniline film is formed. As a result of the previous reaction, a layer of black oxide film can be observed on the electrode surface after the end of the cyclic voltammetry reaction. Figure 6b is the open circuit potential diagram of a polyaniline film prepared in different concentrations of sodium phenyloxalate solution. The downward trend of the open circuit potential in the figure is the same as that of the polyaniline film formed in the previous experiment. Although the slow scanning film forming speed is very slow, the compactness of the film is still not significantly improved. From the final stable open circuit potential, the effect of sodium oxalate concentration is also basic. The disappearance shows that the effect of slow scanning on the density of oxalate has little effect on the aniline film.

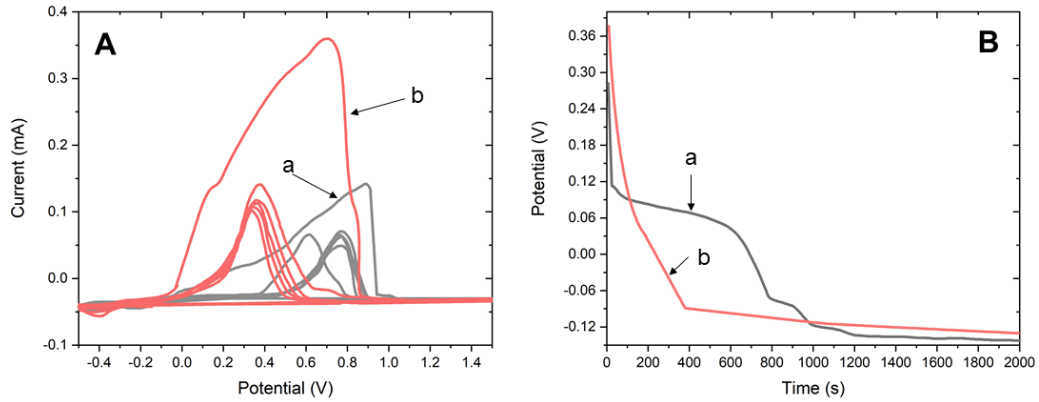

Figure 6. (A) CV curves and (B) open circuit potential of polyaniline films prepared by slow scanning in different concentrations of sodium aniline oxalate solution at 5 mV/s: (a) 0.05 M sodium oxalate+0.1 M aniline and (b) 0.2 M sodium oxalate+0.15 M aniline.

Figure 7 shows the Nyquist diagram and potentiodynamic polarization curves of polyaniline film prepared in the 3% NaCl aqueous solution with different concentrations of aniline oxalate. It can be seen from the diagram that the impedance and potentiodynamic polarization curves of the two different films are basically the same. The film resistance shown by the impedance is basically the same, and the potentiodynamic polarization curve is basically reconnected, which shows that the corrosion resistance of the two films is the same. There is a deviation from a perfect semicircle in the form of a depressed semicircle in the center under the real axis that is due to the state of the electrode surface and the dispersion effect; the above deviation is a typical impedance feature of carbon steel electrodes in a corrosion process [67,68]. The resistance shown by the impedance is less than 1000 ohms, which is the same. The potentiodynamic polarization curve shows that the potential of self-corrosion is close to - 200 mV, and the logarithm of the self-corrosion current is close to - 8.5, which indicates that the corrosion

resistance of the polymer film cannot be obviously improved even if it is formed slowly by slow scanning. Therefore, the polyaniline film only performs as a temporary physical barrier on copper, and the physical barrier effect decreases rapidly with increasing immersion time.

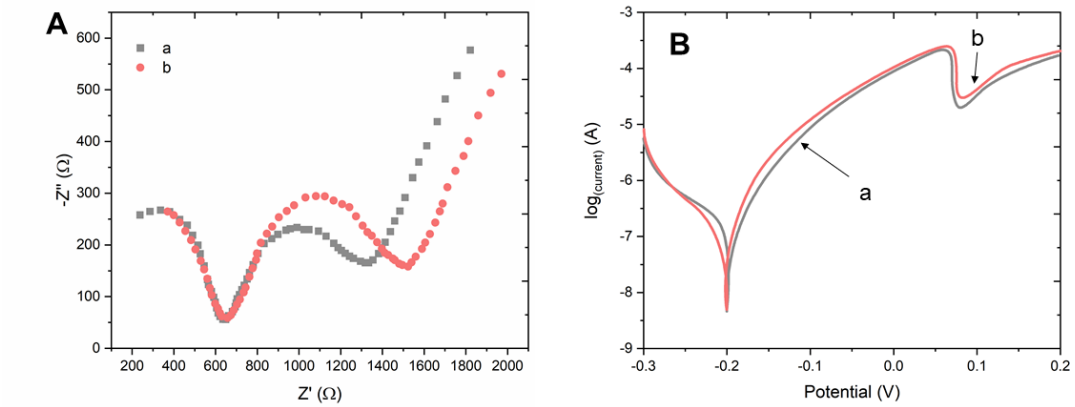

Figure 7. (A) Nyquist plots (amplitude: 10 mV; stabilization period: 1800 s) and (B) potentiodynamic polarization curves (scan rate: 0.5 mV/s) of the polyaniline films prepared by slow scanning in different concentrations of sodium aniline oxalate solution at 5 mV/s: (a) 0.05 M sodium oxalate+0.1 M aniline and (b) 0.2 M sodium oxalate+0.15 M aniline.

4. CONCLUSION

Sodium oxalate can form a layer of insoluble copper oxalate on the surface of copper, which can passivate the surface of copper together with a copper oxide, but the porous density of the film is poor. Aniline cannot be polymerized directly on the copper electrode. However, in a solution containing sodium oxalate, aniline can polymerize on the copper surface and block the formed porous copper oxalate film, thus making the copper surface passivate to a high degree. However, the stability of this passivation is very poor, and it loses its protective effect after soaking in brine for a certain time. This may be related to the poor adhesion between the oxalate copper base and the copper surface. A decrease in scan rate cannot improve the stability of the polyaniline film, which shows that the film can only provide a physical barrier with a weak binding force on the electrode.

References

1. S. Ganiyu, O. Olurin, K. Ajibodu, B. Badmus, A. Ajayi, *Environ. Earth Sci.*, 77 (2018) 443.
2. A. AïtAghzzaf, B. Rhouta, E. Rocca, A. Khalil, *Corros. Sci.*, 114 (2017) 88–95.
3. F. Xie, X. Li, D. Wang, M. Wu, D. Sun, *Eng. Fail. Anal.*, 91 (2018) 382–396.
4. Y. Li, D. Xu, C. Chen, X. Li, R. Jia, D. Zhang, W. Sand, F. Wang, T. Gu, *J. Mater. Sci. Technol.*, 34 (2018) 1713–1718.
5. S. Grousset, M. Bayle, A. Dauzeres, D. Crusset, V. Deydier, Y. Linard, P. Dillmann, F. Mercier-Bion, D. Neff, *Corros. Sci.*, 112 (2016) 264–275.
6. A. Susanto, D.A. Koleva, K. van Breugel, *J. Adv. Concr. Technol.*, 15 (2017) 627–643.
7. S.A. Miran, Q. Huang, H. Castaneda, *J. Infrastruct. Syst.*, 22 (2016) 04016019.

8. O. Andreikiv, I.Y. Dolins'ka, A. Lysyk, N. Sas, *Mater. Sci.*, 52 (2017) 714–721.
9. M. Stechyshyn, N. Stechyshyna, V. Kurskoi, *Mater. Sci.*, 53 (2018) 724–731.
10. B. Hu, R. Yu, J. Liu, *Anti-Corros. Methods Mater.*, 63 (2016) 262–268.
11. N.N. Bin Muhd Noor, K. Yu, U. Bharadwaj, T. Gan, *Mater. Corros.*, 69 (2018) 1237–1256.
12. M. Goyal, S. Kumar, I. Bahadur, C. Verma, E.E. Ebenso, *J. Mol. Liq.*, 256 (2018) 565–573.
13. A. Kalinina, S.Y. Radostin, S.Y. Chloponin, T. Sokolova, A. Moskvichev, E. Razov, V. Kartashov, *Prot. Met. Phys. Chem. Surf.*, 52 (2016) 1193–1196.
14. H. Yu, L. Ma, Z. Li, R. Jiang, *Int. J. Electrochem. Sci.*, 13 (2018) 9416–9427.
15. F. Beshkar, H. Khojasteh, M. Salavati-Niasari, *Materials*, 10 (2017) 697.
16. N. Aravindan, M. Sangaranarayanan, *Prog. Org. Coat.*, 95 (2016) 38–45.
17. J. Wu, C. Cai, Z. Zhou, H. Qian, F. Zha, J. Guo, B. Feng, T. He, N. Zhao, J. Xu, *J. Colloid Interface Sci.*, 463 (2016) 214–221.
18. S. Khamseh, E. Alibakhshi, M. Mahdavian, M.R. Saeb, H. Vahabi, N. Kokanyan, P. Laheurte, *Surf. Coat. Technol.*, 333 (2018) 148–157.
19. M. Ates, *J. Adhes. Sci. Technol.*, 30 (2016) 1510–1536.
20. Z. Grubač, I.Š. Rončević, M. Metikoš-Huković, *Corros. Sci.*, 102 (2016) 310–316.
21. Y. Jafari, S.M. Ghoreishi, M. Shabani-Nooshabadi, *J. Polym. Res.*, 23 (2016) 91.
22. T. Pan, X. Zuo, T. Wang, J. Hu, Z. Chen, Y. Ren, *J. Power Sources*, 302 (2016) 180–188.
23. M.A. Hussein, S.S. Al-Juaid, B.M. Abu-Zied, A.-E.A. Hermas, *Int. J. Electrochem. Sci.*, 11 (2016) 3938–3951.
24. L. Jiang, J.A. Syed, Y. Gao, H. Lu, X. Meng, *Appl. Surf. Sci.*, 440 (2018) 1011–1021.
25. Y. Zhao, Z. Zhang, L. Yu, *React. Funct. Polym.*, 102 (2016) 20–26.
26. P. Li, X. Ding, Z. Yang, M. Chen, M. Wang, X. Wang, *Ionics*, 24 (2018) 1129–1137.
27. Z. Cao, Y. Xia, C. Chen, *Tribol. Int.*, 120 (2018) 446–454.
28. Z.H. Zhang, D.Q. Zhang, L.H. Zhu, L.X. Gao, T. Lin, W.G. Li, *J. Coat. Technol. Res.*, 14 (2017) 1083–1093.
29. K. Cai, S. Zuo, S. Luo, C. Yao, W. Liu, J. Ma, H. Mao, Z. Li, *RSC Adv.*, 6 (2016) 95965–95972.
30. T. Pan, Q. Yu, *Anti-Corros. Methods Mater.*, 63 (2016) 360–368.
31. A.A. Salem, B.N. Grgur, *Int J Electrochem Sci*, 12 (2017) 8683–94.
32. A. Ammar, M. Shahid, M. Ahmed, M. Khan, A. Khalid, Z. Khan, *Materials*, 11 (2018) 332.
33. L. Pan, W. Ding, W. Ma, J. Hu, X. Pang, F. Wang, J. Tao, *Mater. Des.*, 160 (2018) 1106–1116.
34. A. da S. Sirqueira, D. Teodoro Júnior, M. da S. Coutinho, S. Neto, A. dos A. Silva, B.G. Soares, *Polímeros*, 26 (2016) 215–220.
35. R.D.V. Cepeda, R. López-García, R. Mata-González, M. Márquez-Madrid, F. Blanco-Macías, *J Prof Assoc Cactus Dev*, 20 (2019) 151–161.
36. M. Mendoza-Orozco, I. Hernández-Ríos, F. Morales-Flores, J. Mena-Covarrubias, J. Ortega-Espinoza, C. Mondragón-Jacobo, S. de J. Mendez-Gallegos, *J Prof Assoc Cactus Dev*, 20 (2018) 52–67.
37. H. Abrha, E. Birhane, A. Zenebe, H. Hagos, A. Girma, E. Aynekulu, A. Alemie, *J Prof Assoc Cactus Dev*, 20 (2018) 128–150.
38. L. Miranda-Romero, P. Vazquez-Mendoza, J. Burgueño-Ferreira, G. Aranda-Osorio, *J. Prof. Assoc. Cactus Dev.*, 20 (2018) 196–215.
39. B. Quiroz-González, M. García-Mateos, J. Corrales-García, M. Colinas-León, *J. Prof. Assoc. Cactus Dev.*, 20 (2018) 82–100.
40. S.K. Nadaf, M. Safa'a, S.A. Al-Farsi, A.S. Al-Hinai, *J. Prof. Assoc. CACTUS Dev.*, 20 (2018) 68–81.
41. P. Felker, R. Bunch, J.A. Tine, G.R. Russo, J. Gould, M. Arnold, F. Wang, Y. Rong, M. Wright, *J Prof Assoc Cactus Dev*, 20 (2018) 34–51.
42. E. Salazar-Sosa, H.I. Trejo-Escareño, I. Orona-Castillo, E. Salazar-Melendez, L.G. Hernández-Montiel, B. Murillo-Amador, *J Prof Assoc Cactus Dev*, 20 (2018) 1–22.

43. Z. Li, Y. Shen, Y. Li, F. Zheng, L. Liu, *Polym. Int.*, 67 (2018) 121–126.
44. M.G. Hosseini, *Prog. Color Color. Coat.*, 10 (2017) 181–192.
45. T. Pan, T. Wang, *J. Chin. Soc. Corros. Prot.*, 34 (2014) 489–494.
46. P.P. Deshpande, A.A. Bhopale, V.A. Mooss, A.A. Athawale, *Chem. Pap.*, 71 (2017) 189–197.
47. R. Layeghi, M. Farbodi, N. Ghalebsaz-Jeddi, *Int. J. Nanosci. Nanotechnol.*, 12 (2016) 167–174.
48. S. Kim, T.-H. Le, C.S. Park, G. Park, K.H. Kim, S. Kim, O.S. Kwon, G.T. Lim, H. Yoon, *Sci. Rep.*, 7 (2017) 15184.
49. N. Harfouche, N. Gospodinova, B. Nessark, F.X. Perrin, *J. Electroanal. Chem.*, 786 (2017) 135–144.
50. K.M. Košiček, K. Kvastek, V. Horvat-Radošević, *J. Solid State Electrochem.*, 20 (2016) 3003–3013.
51. X. Hou, Y. Wang, G. Sun, R. Huang, C. Zhang, *High Perform. Polym.*, 29 (2017) 305–314.
52. A.S. Ahammad, A. Al Mamun, T. Akter, M. Mamun, S. Faraezi, F. Monira, *J. Solid State Electrochem.*, 20 (2016) 1933–1939.
53. C. De León-Almazán, E. Onofre-Bustamante, J. Rivera-Armenta, M.Á. San Martín, M. Chávez-Cinco, N. Gallardo-Rivas, U. Páramo-García, *Polym. Bull.*, 74 (2017) 1145–1155.
54. J.A. Syed, S. Tang, X. Meng, *Sci. Rep.*, 7 (2017) 4403.
55. M.E. Nicho, H Hu, J.G. Gonzalez-Rodriguez, V.M. Salinas Bravo, *J. Appl. Electrochem.*, 36 (n.d.) 153–160.
56. R. Abdel-Hamid, E.F. Newair, M.K. Rabia, *J. Int. Environ. Appl. Sci.*, 5 (2010) 342–356.
57. T. Jin, Y. Wang, H. Yin, X. Hao, *J. Nanosci. Nanotechnol.*, 18 (2018) 4992–5000.
58. M. Shabani-Nooshabadi, E. Allahyary, Y. Jafari, *J. Nanostructures*, 8 (2018) 131–143.
59. O. Kazum, M.B. Kannan, *Surf. Eng.*, 32 (2016) 607–614.
60. M. Khan, A. Amari, A. Mustafa, H. Shoukry, I.H. Ali, S.A. Umoren, A.M. Kumar, *Int J Electrochem Sci*, 13 (2018) 7385–7396.
61. A. Kausar, *Int. J. Polym. Anal. Charact.*, 22 (2017) 557–567.
62. S.T. Döşlü, B.D. Mert, B. Yazıcı, *Arab. J. Chem.*, 11 (2018) 1–13.
63. S. Kadapparambil, K. Yadav, M. Ramachandran, N.V. Selvam, *Corros. Rev.*, 35 (2017) 111–121.
64. F. Taghipoor, D. Semnani, E. Naghashzargar, B. Rezaei, *J. Compos. Mater.*, 51 (2017) 3355–3363.
65. J. Liu, Y. Lei, Z. Qiu, D. Li, T. Liu, F. Zhang, S. Sun, X. Chang, R. Fan, Y. Yin, *J. Electrochem. Soc.*, 165 (2018) C878–C889.
66. Milica M. Popovi?, Branimir N. Grgur, *Synth. Met.*, 143 (n.d.) 0–195.
67. R.S. Silva, C.A. Ferreira, J.Z. Ferreira, Álvaro Meneguzzi, *Mater. Sci. Forum*, 805 (2014) 155–160.
68. A. Mostafaei, F. Nasirpouri, *Br. Corros. J.*, 48 (2013) 513–524.